Chinese Chemical Letters 36 (2025) 110310

Contents lists available at ScienceDirect

Chinese Chemical Letters

journal homepage: www.elsevier.com/locate/cclet

Chiroptical sensing for remote chiral amines *via* a C–H activation reaction

Xin Li, Jia-Min Lu, Bo Li, Chen Zhao, Bei-Bei Yang, Li Li*

State Key Laboratory of Digestive Health, Beijing Key Laboratory of Active Substances Discovery and Druggability Evaluation, Institute of Materia Medica, Chinese Academy of Medical Sciences & Peking Union Medical College, Beijing 100050, China

ARTICLE INFO

Article history:
Received 16 March 2024
Revised 16 July 2024
Accepted 31 July 2024
Available online 2 August 2024

Keywords:
Electronic circular dichroism (ECD)
Remote chiral amines
C–H activation
Cyclo-palladium
Absolute optical purity

ABSTRACT

An electronic circular dichroism (ECD)-based chiroptical sensing method has been developed for β- and γ-chiral primary amines *via* a C–H activation reaction. With the addition of $Pd(OAc)_2$, the flexible remote chiral primary amine fragment in the bidentate ligand intermediate was fixed to form a cyclopalladium complex, producing an intense ECD response. The correlation between the sign of Cotton effects and the absolute configuration of substrates was proposed, together with theoretical verification using time-dependent density functional theory (TDDFT). Chiroptical sensing of an important drug raw material was performed to provide rapid and accurate information on the absolute optical purity. This work introduces an alternative perspective of C–H activation reaction as well as a feasible chiroptical sensing method of remote chiral amines.

The significance of chirality in medicinal chemistry has been widely acknowledged due to the potential dramatic variations in physiological activity and toxicity between stereoisomers [1–3]. This phenomenon has continuously stimulated interest in developing convenient and reliable chiral analysis methods. The commonly used techniques for determining the absolute configuration of chiral molecules include X-ray single-crystal diffraction, nuclear magnetic resonance (NMR), and chiroptical spectroscopy, such as electronic circular dichroism (ECD) and vibrational circular dichroism (VCD) [4–9].

Chiral small molecule drugs account for more than 50% of the top 200 small molecule drugs by sale in 2022. Remote chiral amines, in which the chiral center is separated from the amine group by one or more carbon atoms, frequently appear in small molecule drugs such as lurasidone and rivaroxaban (Fig. 1). Moreover, several drug candidates under development, including KI-301670, also possess remote chiral amine fragments [10].

Chiral transmission often occurs between small molecules at adjacent spaces through intermolecular forces, which results in the generation of new stereocenters in the reaction products. Therefore, remote chirality plays an important role in asymmetric synthesis reactions [11,12]. However, because the chiral center is not directly connected to the functional group, it is challenging to establish the absolute configuration of remote stereocenters. Only a few reports on remote chiral sensing methods, mainly using NMR or ECD as the analysis tools, have been published. Nikolai's team developed a selenium-based chiral chemical probe that showed high efficiency for accessing remote chiral carboxylic acids *via* ^{77}Se NMR spectroscopy [13]. TBP3 tweezers were suitably introduced to the structure of β-, γ-, or δ-chiral carboxylic acids, yielding typical exciton coupling circular dichroism (ECCD) signals [14]. For α-, β-, and some γ-chiral carboxylic acids, ECCD was also generated by forming a Cu(II)-coordination complex to distort the associated quinolines [15,16]. Additionally, Anslyn's team developed a four-component assembly to perform chiroptical sensing of various β-chiral primary alcohols *via* ECCD [17].

In addition to being important chiral precursors of drugs, chiral amines are often used as key chiral ligands in asymmetric catalytic synthesis [18–20]. This in turn inspired the development of chiral amine sensing methods. Unfortunately, to our knowledge, specific systematic chiroptical sensing of remote chiral amines has not been reported. Thus, there is an urgent need to develop novel chiral sensing methods for remote chiral amines. Because of its convenience, accuracy and efficiency, ECD spectroscopy has gained popularity in this field. In the past decade, considerable progress has been made in ECD-based chiroptical sensing [21–26]. It is feasible and meaningful to establish a reliable ECD method to analyze the absolute optical purity of remote chiral amines.

In a typical C–H activation reaction, C-X (X = C, N, O, *etc.*) bond coupling is realized through cleavage of the C–H bond catalyzed by a transition metal complex [27–32]. This class of reactions is

* Corresponding author.
E-mail address: annaleelin@imm.ac.cn (L. Li).

https://doi.org/10.1016/j.cclet.2024.110310
1001-8417/

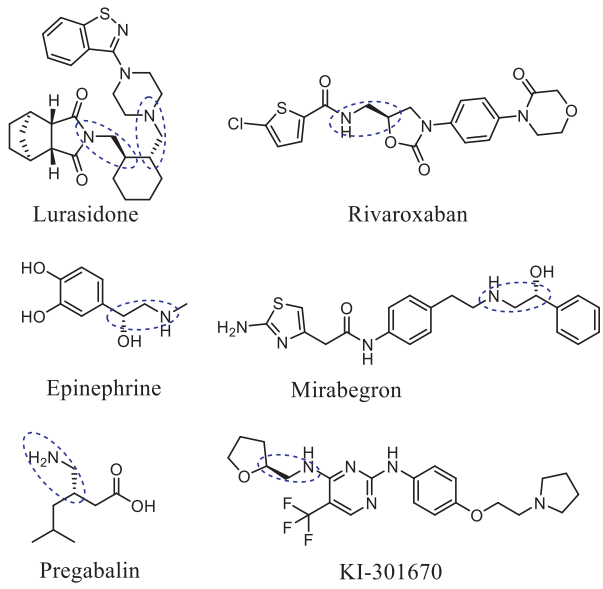

Fig. 1. Typical drugs containing remote chiral amine fragments.

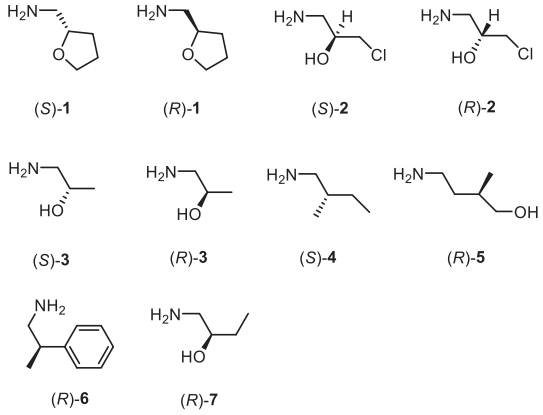

Fig. 2. Typical primary amines with remote stereocenters.

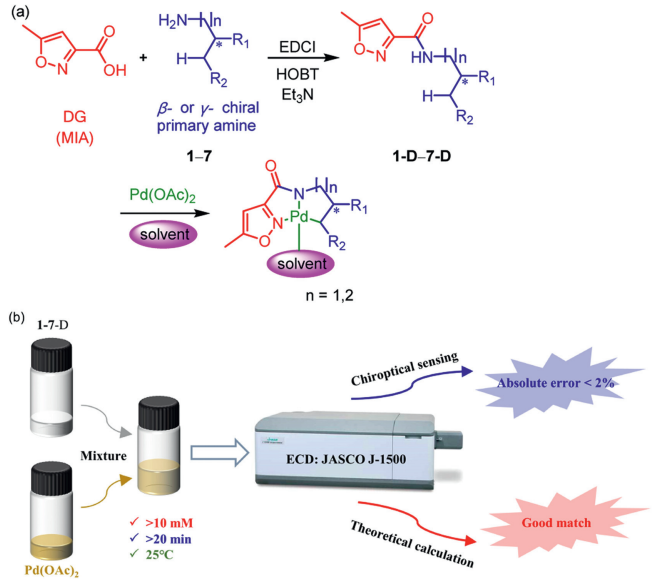

Scheme 1. (a) Synthesis route of cyclopalladium complexes. (b) Schematic illustration of remote chiroptical sensing of β- or γ-primary amines.

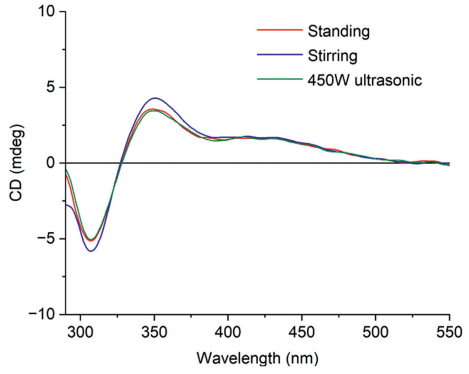

Fig. 3. ECD spectra of the (*R*)-**1-D** Pd complex in HFIP under different reaction modes, standing or stirring at room temperature, and promotion by 450 W of ultrasonication. ECD measurements were conducted with 6 mmol/L samples in a 1 mm cuvette.

atom-economical and has been widely applied to construct various skeleton compounds [33,34]. Here, we report a rapid and accurate chiroptical sensing method for remote chiral amines *via* a C–H activation reaction using 5-methylisoxazole-3-carboxylic acid (MIA) as the directing group [35,36].

Several β- or γ-chiral primary amines were condensed with MIA to yield bidentate ligands (**1-*D*–7-D**, Fig. 2). The Pd atom was then introduced by binding the directing group and activating the target C–H bond to form a double five-membered or mixed five-membered or six-membered cyclopalladium complex (Scheme 1). This Pd complex was absorbed in the ultraviolet–visible range, and Cotton effects (CEs) were induced when this chromophore was disturbed by the chirality of the chiral amines. The ECD spectra of the cyclopalladium complexes were calculated theoretically and were in good agreement with the experimental results. Samples with different enantiomeric excess (*ee*) values were prepared for the absolute optical purity test, with an absolute error less than 2%. Considering the great progress in the field of Pd-catalyzed C–H activation reactions [37–40], the strategy of using a Pd chromophore to determine the absolute optical purity of chiral molecules is promising.

The sensing reaction was first attempted for (*R*)–**1-D** in 1,1,1,3,3,3-hexafluoro-2-propanol (HFIP), which is often used in C–H activation reactions. Two equivalents of $Pd(OAc)_2$ were added, the reaction concentration was 10 mmol/L, and the reaction time was 20 min. Three reaction modes were compared: promotion by 450 W ultrasound, standing or stirring at room temperature (Fig. 3). The difference between these reaction modes was small, indicating that the reaction mode had little effect on this reaction. For the convenience of operation, the reaction mixture was allowed to stand at room temperature.

The sensing reaction was then evaluated in eight frequently used solvents for the C–H activation reaction, namely, HFIP, 2,2,2-trifluoroethanol (TFE), acetonitrile (ACN), *tert*–butanol (TBA), 1,4-dioxane (Dx), 1,2-dimethoxyethane (DME), 1,2-dichloro-ethane (DCE), and acetic acid (AcOH). Unexpectedly, the solvent affected the position and intensity of the Cotton effect in the ECD spectra (Fig. 4). This fact might be attributed to the solvation effects on the ECD signals as well as the possible participation of the solvent molecule in the cyclopalladium complex. Much more intense ECD responses appeared for HFIP, TFE, ACN, and TBA. In particular, the highest intensity of Cotton effects was observed in TFE, while TBA was not suitable as a reaction solvent because of the poor solubility of $Pd(OAc)_2$ in this solvent.

The time required for the reaction to reach a steady state depended on the reactant concentration. Time curves of the ECD signal at 324 nm in TFE were obtained at reactant concentrations of

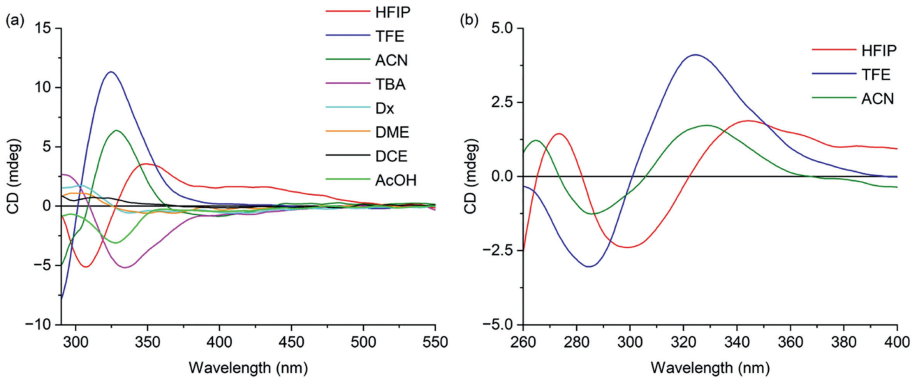

Fig. 4. ECD responses of (*R*)-**1-D** sensing solutions in different solvents. (a) Samples were reacted at a concentration of 10 mmol/L for 20 min and diluted to 6 mmol/L for ECD measurements. (b) Samples were reacted at a concentration of 20 mmol/L for 20 min and then diluted to 2 mmol/L for ECD measurements.

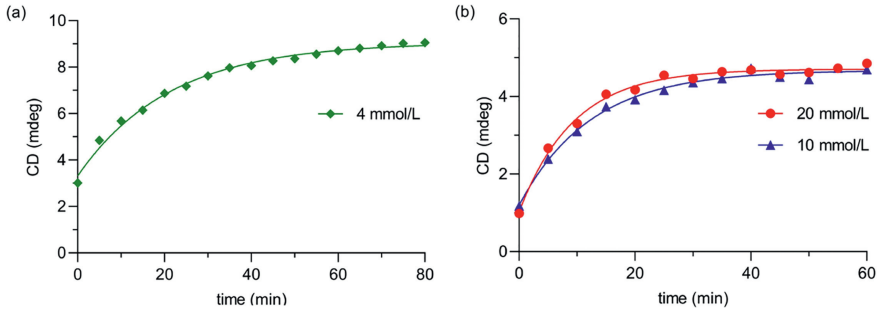

Fig. 5. Time curves of the ECD signals at 324 nm for different reactant concentrations. (a) The reaction and ECD concentration were 4 mmol/L, and ECD spectra were collected every 5 min for 80 min. (b) The reaction concentration was 10 or 20 mmol/L, and ECD measurements were conducted at 2 mmol/L every 5 min for 60 min. Nonlinear curve fitting was performed using GraphPad Prism 8.

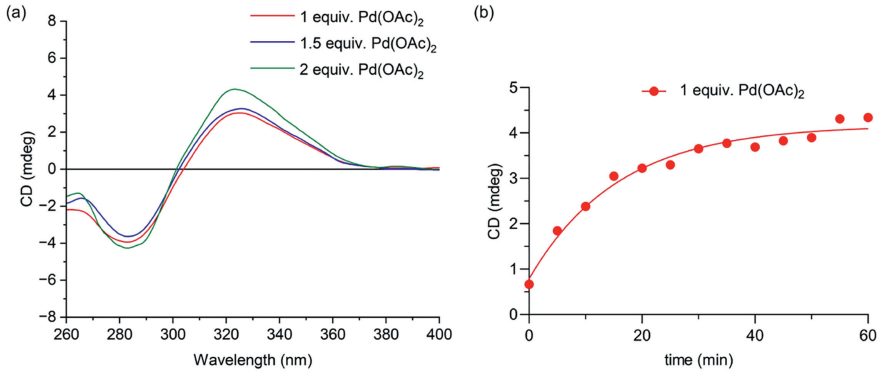

Fig. 6. Optimization of the molar ratio of $Pd(OAc)_2$ to (*R*)-**1-D**. (a) ECD spectra of the reaction mixture at different molar ratios. (b) Time curve of ECD signals at 324 nm with an equivalence ratio of $Pd(OAc)_2$ to (*R*)-**1-D**. ECD spectra were measured at 2 mmol/L. Nonlinear curve fitting was performed using GraphPad Prism 8.

4, 10, and 20 mmol/L (Fig. 5). When the reactant concentration was set to 4 mmol/L, the reaction did not reach a relatively steady state until 80 min. However, when the reactant concentration increased to 10 mmol/L or 20 mmol/L, the reaction reached a steady state within 20 min. Therefore, the concentration needed to be greater than 10 mmol/L, and the optimal test time was 20 min or longer to ensure that the reaction had completely occurred.

A greater amount of $Pd(OAc)_2$ promoted the chiroptical sensing process; however, excess $Pd(OAc)_2$ exhibited strong UV absorption within the tested wavelength range, reducing the signal-to-noise ratio in the ECD spectra. The molar ratios of $Pd(OAc)_2$ to (*R*)-**1-D** were thus set as 1:1, 1.5:1, and 2:1 in TFE when chiroptical sensing occurred at room temperature and was monitored at 20 min. As shown in Fig. 6a, the intensity of the Cotton effect at 324 nm increased slightly with the amount of $Pd(OAc)_2$. However, the reaction did not reach a relatively steady state within 60 min for the reaction mixture with a molar ratio of $Pd(OAc)_2$ to (*R*)-**1-D** of 1:1 (Fig. 6b). Thus, 2 equiv. of $Pd(OAc)_2$ were added for subsequent tests, considering the reaction efficiency and the reliability of the ECD signal.

Adopting the established sensing conditions, the substrate range for remote chiroptical sensing was extended to ten commercially available β- or γ-chiral primary amines, including three pairs of enantiomers and four single enantiomers (Fig. 2). As expected, all the sensing mixtures displayed obvious ECD responses over the wavelength range from 250 nm to 550 nm (Fig. 7 and Table S1 in Supporting information).

Based on the sensing results, the relationship between the absolute configuration of these β- and γ-chiral amines and the ECD signals was investigated. Similar to the bulkiness rule of the $[Rh_2(CF_3COO)_4]$ complex for chiral alcohols [41], the Cotton effect was found to depend on the group arrangement of these sensing

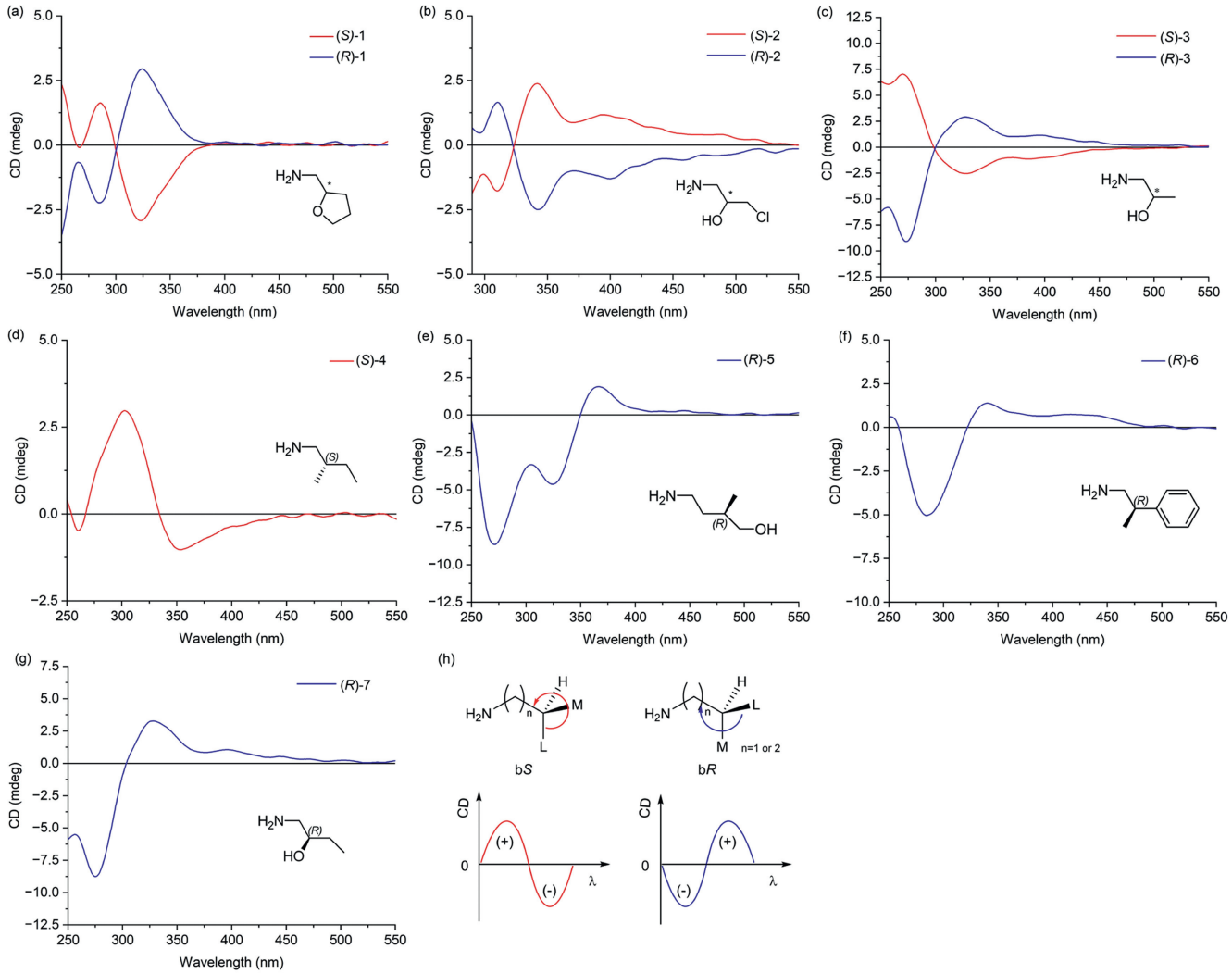

Fig. 7. ECD spectra of sensing solutions of the tested remote chiral primary amines (a-g) and schematic diagram of the correlation between the sign of the Cotton effect and the absolute configuration of the substrates (h). Chiroptical sensing occurred at a concentration of 20 mmol/L for 20 min, and ECD measurements were conducted with samples diluted to 2 mmol/L.

products. First, the amino group fragments were fixed, and then the remaining three groups were arranged in order of decreasing volume. If the order is clockwise, the configuration is b*R*; if the order is counterclockwise, the configuration is b*S*. Stereoisomers with a b*R* configuration showed a positive Cotton effect followed by a negative Cotton effect from long to short wavelengths, and *vice versa* for a b*S* isomer. Moreover, the wavelength at which the substituent crossed the zero point varied with the substituent. When a carbon or oxygen atom is connected at the α or β position of the carbon stereocenter ((*R*/*S*)-**1**, (*R*/*S*)-**3**, (*S*)-**4**, (*R*)-**5**, (*R*)-**6**, or (*R*)-**7**), the b*R*/b*S* configuration corresponds to the *R*/*S* configuration. However, in the case of (*R*/*S*)-**2**, the b*S* configuration corresponds to the *R* configuration due to the higher priority of the chlorine atom. Chiroptical sensing of the chiral drug fragment atorvastatin intermediate **1** was performed, and the signal of the Cotton effect conformed to the rules we summarized (Fig. S1 in Supporting information). Due to the limited number of compounds attempted, a comprehensive correlation requires further research.

The ECD spectra of several cyclopalladium complexes were theoretically predicted by using time-dependent density functional theory (TDDFT) with a solvation model based on density (SMD) [42]. The calculated ECD spectra of the (*S*)-**1-D**-Pd, (*R*)-**2-D**-Pd, and (*S*)-**4-D**-Pd complexes agreed well with the experimental ECD spectra (Fig. 8a and Fig. S3 in Supporting information). Natural transition orbital (NTO) analysis of the cyclopalladium complex was performed using Multiwfn 3.8 [43]. The results indicated that the d orbitals of the Pd atom participated substantially in the NTO pairs related to the S0→S2 and S0→S6 transitions (Fig. 8b).

To confirm the structure of the sensing product, single-crystal X-ray diffraction analysis was performed. We obtained a single crystal (CCDC: 2289496), which was proven to be stable dimerization complex **8** (Fig. 9 and Table S2 in Supporting information), without the anticipated C-Pd bond.

Comparing the ECD spectra of **8** and the chiroptical sensing mixture of (*S*)-**4-D**, it is obvious that compound **8** displayed different ECD patterns and weaker ECD signals than the chiroptical sensing product, indicating their structural differences. Importantly, the ECD spectrum of compound **8** lacked a negative Cotton effect at approximately 350 nm, which could be attributed to the existence of a C-Pd bond.

Chiral 2-tetrahydrofurfurylamine ((*R*/*S*)-**1**, Fig. 2) is a notable raw material and acts as a chiral source for some drugs or drug candidates (Fig. S5 in Supporting information). For the NUAK1 inhibitor KI-301670 (Fig. 1), which is a promising drug candidate against pancreatic cancer, the *S* isomer is the eutomer [10]. The stereochemical configuration of the 2-tetrahydrofurfurylamine

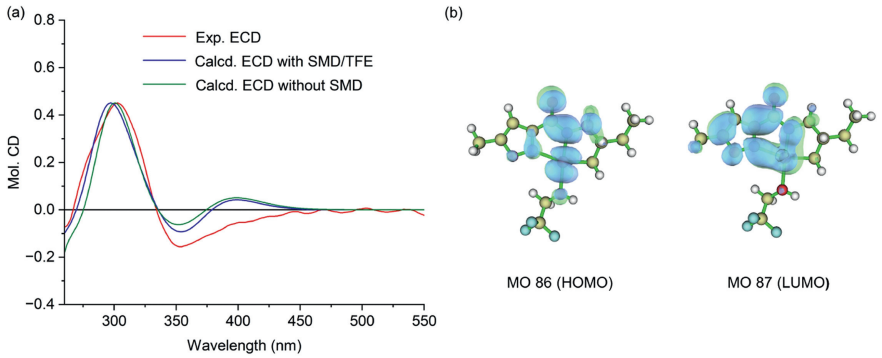

Fig. 8. (a) Comparison of the experimental and calculated ECD spectra of the (*S*)-**4-D**-Pd complex with SMD/TFE or without SMD. (b) NTOs for the (*S*)-**4-D**-Pd complex, with an isovalue of 0.02. The calculated ECD spectra were generated using SpecDis 1.71 software [44].

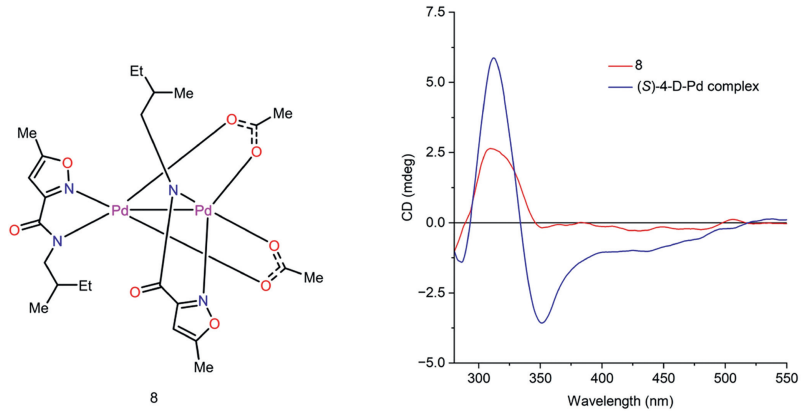

Fig. 9. ECD spectra of compound **8** and the (*S*)–**4-D**-Pd complex in dichloromethane.

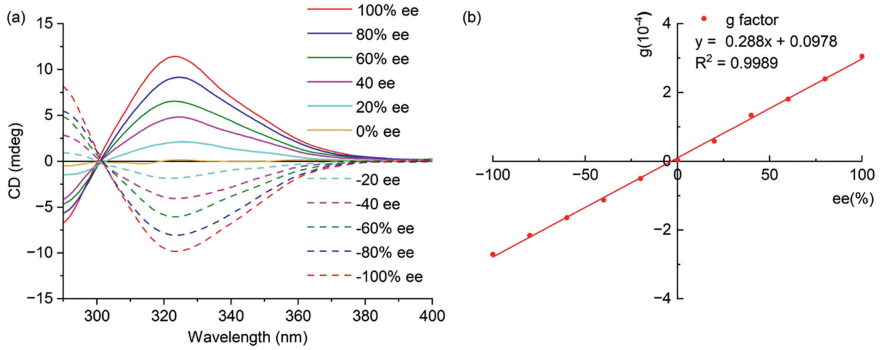

Fig. 10. ECD spectra and calibration curves of *ee* for (*R*/*S*)-**1-D**. (a) ECD spectra of (*R*/*S*)-**1-D** with different *ee* values. (b) Calibration curves between the g-factor at 324 nm and *ee* of (*R*/*S*)-**1-D**. Samples were reacted at 10 mmol/L for 30 min and measured at 5 mmol/L for ECD. Herein, the *ee* was defined as (*R*-*S*)/(*R* + *S*) × 100%.

fragment strongly affected the interaction with the target protein, and the *S* configuration was necessary for hydrophobic interactions with the Leu185 residue in the protein binding pocket.

Herein, the absolute optical purity of (*R*/*S*)-**1** was evaluated using the established chiroptical sensing protocol. To avoid the impact of sampling concentration fluctuations, the anisotropy factor (g-factor) was selected as the evaluation index for absolute optical purity. For (*R*/*S*)-**1-D**, a good linear correlation was obtained when the g-factors at 324 nm in TFE were plotted against the *ee* values (Fig. 10).

Subsequently, five samples with different *ee* values were prepared for chiroptical sensing analysis, and the detection error was less than 2% (Table 1). Chiroptical sensing was also tested in HFIP, and the results are listed in Fig. S4 and Table S5 (Supporting information). These results support the feasibility and reliability of the chiroptical sensing method.

Table 1
Chiroptical sensing results for (*R*/*S*)-**1-D**.

Entry	Actual *ee* values (%)	Sensing results (%)	Absolute error (%)
1	76.00	75.58	0.42
2	48.00	46.82	1.18
3	18.00	16.06	1.94
4	−46.00	−47.92	1.92
5	−86.00	−87.15	1.15

In conclusion, a rapid and accurate chiroptical sensing protocol for remote chiral primary amines was established by combining a powerful C–H activation reaction and a specific ECD technique. For these β- or γ-chiral primary amines, the absolute configurations could be unambiguously assigned by constructing cyclopalladium metal complexes. ECD test samples were taken directly from the

reaction solution without tedious post-treatment, and a detection error of less than 2% was achieved. This work is an innovative attempt at the application of the C–H activation reaction to determine the absolute optical purity of remote chiral small-molecule compounds. With the continuous development of novel C–H activation reactions, further research is underway for more chiral structures and for monitoring asymmetric synthetic reactions.

Declaration of competing interest

The authors declare that they have no known competing financial interests or personal relationships that could have appeared to influence the work reported in this paper.

CRediT authorship contribution statement

Xin Li: Writing – original draft, Methodology, Investigation, Data curation. **Jia-Min Lu:** Methodology, Investigation, Data curation. **Bo Li:** Methodology, Investigation, Data curation, Conceptualization. **Chen Zhao:** Investigation, Data curation. **Bei-Bei Yang:** Validation, Resources, Methodology. **Li Li:** Writing – review & editing, Supervision, Project administration, Funding acquisition, Conceptualization.

Acknowledgments

All quantum computations were carried out using the Gaussian 16 package supported by the Biomedical High Performance Computing Platform, Chinese Academy of Medical Sciences. This work was financially supported by the CAMS Innovation Fund for Medical Sciences (CIFMS, No. 2023-I2M-2-009).

Supplementary materials

Supplementary material associated with this article can be found, in the online version, at doi:10.1016/j.cclet.2024.110310.

References

[1] J. Valentová, L. Lintnerová, N. Miklášová, et al., Int. J. Mol. Sci. 24 (2023) 5679.
[2] D. Saha, A. Kharbanda, W. Yan, et al., J. Med. Chem. 63 (2020) 441–469.
[3] X. Chu, Y. Bu, X. Yang, Front. Oncol. 11 (2021) 785855.
[4] S. Jang, H. Park, Q.H. Duong, et al., Anal. Chem. 94 (2022) 1441–1446.
[5] G. Pescitelli, Chirality 34 (2022) 333–363.
[6] A. Mándi, T. Kurtán, Nat. Prod. Rep. 36 (2019) 889–918.
[7] F. Krupp, W. Frey, C. Richert, Angew. Chem. Int. Ed. 59 (2020) 15875–15879.
[8] M. Chen, C. Qi, Y. Yin, et al., Org. Chem. Front. 9 (2022) 5160–5167.
[9] Y. Wu, P. Wang, L. Zheng, et al., Sensor. Actuat. B: Chem. 380 (2023) 133330.
[10] M.S. Seo, K.H. Jung, K. Kim, et al., Biomed. Pharmacother. 152 (2022) 113241.
[11] P. Linnane, N. Magnus, P. Magnus, Nature 385 (1997) 799–801.
[12] H.Q. Shen, B. Wu, H.P. Xie, et al., Org. Lett. 21 (2019) 2712–2717.
[13] S.A. Shyshkanov, N.V. Orlov, Chem. Eur. J. 22 (2016) 15458–15467.
[14] M. Tanasova, M. Anyika, B. Borhan, Angew. Chem. Int. Ed. 54 (2015) 4274–4278.
[15] L.A. Joyce, J.W. Canary, E.V. Anslyn, Chemistry 18 (2012) 8064–8069.
[16] L.A. Joyce, M.S. Maynor, J.M. Dragna, et al., J. Am. Chem. Soc. 133 (2011) 13746–13752.
[17] M.B. Minus, A.L. Featherston, S. Choi, et al., Chem 5 (2019) 3196–3206.
[18] J. Yang, X.M. Zhang, F.M. Zhang, et al., Angew. Chem. Int. Ed. 59 (2020) 8471–8475.
[19] Z.K. Xue, N.K. Fu, S.Z. Luo, Chin. Chem. Lett. 28 (2017) 1083–1086.
[20] L. Næsborg, V. Corti, L.A. Leth, et al., Angew. Chem. Int. Ed. 57 (2018) 1606–1610.
[21] B. Li, J. Zhang, L. Li, et al., Chem. Sci. 12 (2020) 2504–2508.
[22] S.L. Pilicer, C. Wolf, J. Org. Chem. 85 (2020) 11560–11565.
[23] A. Sripada, F.Y. Thanzeel, C. Wolf, Chem 8 (2022) 1734–1749.
[24] J. Zhang, B. Yang, Y. Yang, et al., Ultrason. Sonochem. 86 (2022) 106007.
[25] K. Ngamdee, W. Ngeontae, Sensor. Actuat. B: Chem. 274 (2018) 402–411.
[26] A. Chen, Y. Zhong, X. Yin, et al., Sensor. Actuat. B: Chem. 393 (2023) 134262.
[27] W. Ali, G. Prakash, D. Maiti, Chem. Sci. 12 (2021) 2735–2759.
[28] G. Liao, T. Zhang, Z.K. Lin, et al., Angew. Chem. Int. Ed. 59 (2020) 19773–19786.
[29] M. Zhang, S. Zhong, Y. Peng, et al., Org. Chem. Front. 8 (2021) 133–168.
[30] Y. Han, B. Shi, Acta Chim. Sinica 81 (2023) 1522–1540.
[31] B. Liu, A.M. Romine, C.Z. Rubel, et al., Chem. Rev. 121 (2021) 14957–15074.
[32] Q. Zhang, B. Shi, Acc. Chem. Res. 54 (2021) 2750–2763.
[33] J. Zhang, B. Lu, Z. Ge, et al., Org. Lett. 24 (2022) 8423–8428.
[34] M. Zheng, J. Zhou, F. Fang, et al., Org. Chem. Front. 10 (2023) 62–67.
[35] K.K. Pasunooti, B. Banerjee, T. Yap, et al., Org. Lett. 17 (2015) 6094–6097.
[36] K.K. Pasunooti, R. Yang, B. Banerjee, et al., Org. Lett. 18 (2016) 2696–2699.
[37] J.M. Gonzalez, X. Vidal, M.A. Ortuno, et al., J. Am. Chem. Soc. 144 (2022) 21437–21442.
[38] J. Wang, D. Hu, X. Sun, et al., Org. Lett. 25 (2023) 2006–2011.
[39] Q. Li, K. Yan, Y. Zhu, et al., Chin. Chem. Lett. 34 (2023) 108014.
[40] Y. Peng, Q. He, X. Zhang, et al., Org. Chem. Front. 6 (2019) 3234–3237.
[41] J. Frelek, W.J. Szczepek, Tetrahedron: Asymmetr. 10 (1999) 1507–1520.
[42] A.V. Marenich, C.J. Cramer, D.G. Truhlar, J. Phys. Chem. B 113 (2009) 6378–6396.
[43] T. Lu, F.Y. Chen, J. Comput. Chem. 33 (2012) 580–592.
[44] T. Bruhn, A. Schaumlöffel, Y. Hemberger, et al., SpecDis Version 1.71, 2017 Berlin, Germany https://specdis-software.jimdo.com .